Available online at www.sciencedirect.com
SCIENCE DIRECT®
Journal of Sound and Vibration 271 (2004) 651–670
JOURNAL OF SOUND AND VIBRATION
www.elsevier.com/locate/jsvi

Free vibration and stability of laminated composite circular arches subjected to initial axial stress

Hiroyuki Matsunaga*

Department of Architecture, Setsunan University, 17-8, Ikeda-nakamachi, Neyagawa, Osaka 572-8508, Japan

Received 23 September 2002; accepted 13 March 2003

Abstract

Natural frequencies and buckling stresses of laminated composite circular arches subjected to initial axial stress are analyzed by taking into account the complete effects of transverse shear and normal stresses and rotatory inertia. By using the method of power series expansion of displacement components, a set of fundamental dynamic equations of a one-dimensional higher order theory for laminated composite circular arches subjected to initial axial stress is derived through Hamilton's principle. Several sets of truncated approximate theories are applied to solve the eigenvalue problems of a simply supported circular arch. In order to assure the accuracy of the present theory, convergence properties of the first four natural frequencies are examined in detail. Numerical results are compared with those of the published existing theories. The present global higher order approximate theories can predict the natural frequencies and buckling stresses of multilayered circular arches accurately with a small number of unknowns.

1. Introduction

Advanced composite materials have new problems, such as effects of transverse shear deformation due to the low ratio of transverse shear modulus to axial modulus, failure due to delamination and other secondary effects in the material formation. For laminated composite curved beams and arches, the dominant effects of transverse shear and normal stresses on the natural frequencies, buckling stresses and interlaminar stresses may be found as in the case of laminated composite beams. Although a number of investigations on the vibration analysis of curved beams made of isotropic materials can be found in the survey studies (e.g., Refs. [1,2]), only very limited references were found on laminated composite curved beams and arches.

*Tel.: +81-72-839-9129; fax: +81-72-838-6599.
E-mail address: matsu@arc.setsunan.ac.jp (H. Matsunaga).

0022-460X/03/$ - see front matter
doi:10.1016/S0022-460X(03)00298-0

The classical laminated arch theory [3], based on the shallow shell theory, has been applied to the vibration problems of simply supported thin arches by using the Ritz method. Since the effects of shear deformation and rotatory inertia are neglected, natural frequencies may be inaccurate for a moderately deep laminated arch with relatively soft transverse shear modulus and for highly anisotropic composites. In order to take into account these effects, the first order shear deformation theory for moderately deep arches has been developed including the z/R term in the fundamental equations by Qatu [4,5]. Based on the Timoshenko-type curved beam theory, the free vibration of laminated composite curved beams with variable curvature has been investigated by Tseng et al. [6]. However, since in these theories the transverse shear strain is assumed to be constant in the depth direction, a shear correction factor has to be incorporated to adjust the transverse shear stiffness. The accuracy of solutions of the first order shear deformation theory and Timoshenko-type theory will be strongly dependent on predicting better estimates for the shear correction factor.

For elastic and isotropic materials, one-dimensional higher order theories which take into account the complete effects of shear deformations and rotatory inertia have been presented by Matsunaga for arches [7] and rings [8]. Natural frequencies and buckling loads of circular arches and rings subjected to concentrated axial forces were analyzed. It has been pointed out that shear deformations have important effect on the natural frequencies and buckling loads of thick arches and rings.

Several approximately refined one-dimensional higher order theories which take into account the effects of transverse shear and normal stresses and rotatory inertia have been proposed to analyze the response characteristics of laminated composite beams. A number of single-layer (global) higher order beam theories that include the effects of transverse shear deformations have been published by Matsunaga [9]. Natural frequencies, buckling stresses and interlaminar stresses of multilayered composite beams have been analyzed by using the one-dimensional global higher order theories. Remarkable effects of transverse shear deformation and depth change have been predicted for the results. It has been shown that a global higher order beam theory can predict accurate results not only for the natural frequency and buckling stress but also for the distribution of displacements and stress components in multilayered composite beams. However, general one-dimensional higher order theories have not been investigated in the vibration and stability problems of multilayered composite arches.

This paper presents a global higher order theory for analyzing natural frequencies and buckling stresses of laminated composite circular arches subjected to initial axial stress. The complete effects of both shear and normal stresses can be taken into account within the approximate one-dimensional theory. Several sets of the governing equations of truncated approximate theories are applied to the analysis of vibration and stability problems of a simply supported multilayered elastic circular arches. Based on the power series expansions of continuous displacement components, a fundamental set of equations of a one-dimensional higher order circular arch theory is derived through Hamilton's principle. Natural frequencies and buckling stresses of a simply supported laminated composite circular arch subjected to initial axial stress are obtained by solving the eigenvalue problems. The modal transverse shear and normal stresses are calculated by integrating the three-dimensional equations of motion in the depth direction, and satisfying the continuity conditions at the interface between layers and stress boundary conditions at the top and bottom surfaces of arches. The one-dimensional global higher order theory in the present

paper can predict natural frequencies and buckling stresses of simply supported multilayered circular arches subjected to initial axial stress accurately within a small number of unknowns.

2. Fundamental equations of laminated composite circular arch

Consider a circular arch of arc length L as shown in Fig. 1, having a thin rectangular cross-section of depth H and width B which is assumed to be sufficiently small relative to the depth. The radius of curvature R of the circular arch is assumed to be sufficiently large relative to the depth (i.e., $H/R \ll 1$). A curvilinear co-ordinate system (x, y, z) is defined on the central axis of the circular arch, where the x-axis is taken along the central axis with the y-axis in the width direction and the z-axis in the direction normal to the tangent to the central axis. Assuming that the deformations of the arch take place in the x–z plane, the displacement components of an arch in the x, y and z directions, respectively, can be expressed as

$$u \equiv u(x, z; t), \qquad v \equiv v(x, z; t) = 0, \qquad w \equiv w(x, z; t). \tag{1}$$

The displacement components may be expanded into power series of the normal co-ordinate z as follows:

$$u = \sum_{n=0}^{\infty} \overset{(n)}{u}\, z^n, \qquad w = \sum_{n=0}^{\infty} \overset{(n)}{w}\, z^n, \tag{2}$$

where $n = 0, 1, 2, \ldots, \infty$.

Based on this expression of the displacement components, a set of the linear fundamental equations of a one-dimensional higher order arch theory can be summarized in the following.

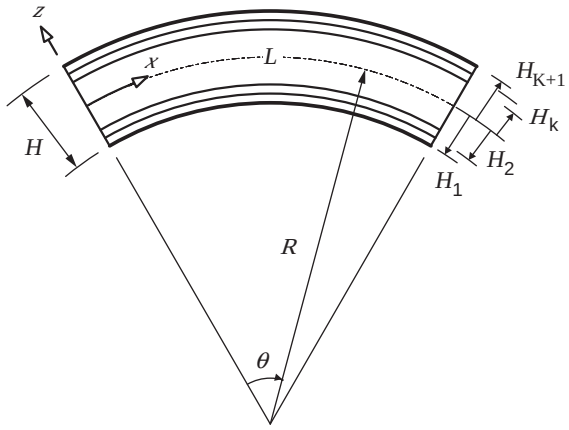

Fig. 1. K-layer laminated composite circular arch and co-ordinates.

2.1. Strain–displacement relations

Strain components may be expanded as follows:

$$\varepsilon_{xx} = \sum_{n=0}^{\infty} \overset{(n)}{\varepsilon}_{xx} z^n, \qquad \varepsilon_{zz} = \sum_{n=0}^{\infty} \overset{(n)}{\varepsilon}_{zz} z^n, \qquad \gamma_{xz} = \gamma_{zx} = \sum_{n=0}^{\infty} \overset{(n)}{\gamma}_{xz} z^n, \tag{3}$$

and strain–displacement relations can be written as [10]

$$\varepsilon_{xx}^{(n)} = \overset{(n)}{u}_{,x} - \frac{1}{R} \overset{(n)}{w}, \qquad \varepsilon_{zz}^{(n)} = (n+1) \overset{(n+1)}{w},$$

$$\gamma_{xz}^{(n)} = \gamma_{zx}^{(n)} = \frac{1}{2}\left\{ (n+1) \overset{(n+1)}{u} - \frac{n-1}{R} \overset{(n)}{u} + \overset{(n)}{w}_{,x} \right\}, \tag{4}$$

where a comma denotes partial differentiation with respect to the co-ordinate subscripts that follow. The curvature parameter is assumed to be $H/R \ll 1$, but no assumption is made for the shallowness parameter L/R.

2.2. Equations of motion and boundary conditions

Under the assumption of plane strain or plane stress in the width direction, by introducing stress components σ_{xx}, $\tau_{xz} = \tau_{zx}$ and σ_{zz}, Hamilton's principle is applied to derive the equations of dynamic equilibrium and natural boundary conditions of an arch. In order to treat vibration and stability problems of an arch subjected to initial axial stress σ_0, additional work due to this stress which is assumed to remain unchanged during vibrating and/or buckling is taken into consideration.

The principle for the present problems may be expressed for an arbitrary time interval t_1 to t_2 as follows:

$$\int_{t_1}^{t_2} \int_V \{\sigma_{xx}\delta\varepsilon_{xx} + 2\tau_{xz}\delta\gamma_{xz} + \sigma_{zz}\delta\varepsilon_{zz} + \sigma_0(u_{,x}\delta u_{,x} + w_{,x}\delta w_{,x}) - \rho(\dot{u}\delta\dot{u} + \dot{w}\delta\dot{w})\} \, \mathrm{d}V \, \mathrm{d}t = 0, \tag{5}$$

where the overdot indicates partial differentiation with respect to time and ρ denotes the mass density; $\mathrm{d}V$, the volume element; $\mathrm{d}S$, the element of area of the external bounding surface.

The initial axial stress σ_0 is assumed to be expanded as follows:

$$\sigma_0 = \sum_{\ell=0}^{\infty} \overset{(\ell)}{\sigma}_0 z^{\ell}, \tag{6}$$

where $\ell = 0, 1, 2, \ldots, \infty$.

By performing the integration over the area of cross-section of the arch and the variation as indicated in Eq. (5), the equations of motion are obtained as follows:

$$\delta \overset{(n)}{u}: \ \overset{(n)}{N}_{,x} - n \overset{(n-1)}{Q} + \frac{(n-1)}{R} \overset{(n)}{Q} + \sum_{m=0}^{\infty} \left[\sum_{\ell=0}^{\infty} \overset{(n+m+\ell+1)}{\sigma_0} \overset{(m)}{u}_{,xx} - \overset{(n+m+1)}{\rho} \overset{(m)}{\ddot{u}} \right] = 0, \tag{7}$$

$$\delta \overset{(n)}{w}: \frac{1}{R}\overset{(n)}{N} + \overset{(n)}{Q}_{,x} - n\overset{(n-1)}{T} + \sum_{m=0}^{\infty}\left[\sum_{\ell=0}^{\infty} \overset{(n+m+\ell+1)}{\sigma_0}\ \overset{(m)}{w}_{,xx} - \overset{(n+m+1)}{\rho}\ \overset{(m)}{\ddot{w}}\right] = 0, \tag{8}$$

where $n, m = 0, 1, 2, \ldots, \infty$ and

$$\overset{(n+m+\ell+1)}{\sigma_0} = \sum_{k=1}^{K} \sigma_0^{(k)} \frac{H_{k+1}^{n+m+\ell+1} - H_k^{n+m+\ell+1}}{n+m+\ell+1},$$
$$\overset{(n+m+1)}{\rho} = \sum_{k=1}^{K} \rho^{(k)} \frac{H_{k+1}^{n+m+1} - H_k^{n+m+1}}{n+m+1}, \tag{9}$$

where $\sigma_0^{(k)}$, $\rho^{(k)}$ and H_k denote the initial axial stress, the mass density of kth layer and the thickness co-ordinate of the lower side of kth layer, respectively, and K denotes the total number of layers in the laminated arches.

The stress resultants are defined as follows:

$$(\overset{(n)}{N}, \overset{(n)}{Q}, \overset{(n)}{T}) = \sum_{k=1}^{K} (\sigma_{xx}^{(k)}, \tau_{xz}^{(k)}, \sigma_{zz}^{(k)}) \frac{H_{k+1}^{n+1} - H_k^{n+1}}{n+1}. \tag{10}$$

The equations of boundary conditions at the ends on the central axis as follows:

$$\overset{(n)}{u} = \overset{(n)}{u^*} \quad \text{or} \quad \overset{(n)}{N} = \overset{(n)}{N^*},$$
$$\overset{(n)}{w} = \overset{(n)}{w^*} \quad \text{or} \quad \overset{(n)}{Q} = \overset{(n)}{Q^*}, \tag{11}$$

where $n = 0, 1, 2, \ldots, \infty$ and the quantities marked with an asterisk denote quantities prescribed at the ends on the central axis of an arch.

2.3. Constitutive relations

For elastic and orthotropic materials of each layer of laminated composite circular arches, the two-dimensional constitutive relations for kth layer can be written under the assumption of plane stress in the width direction of the arch as

$$\begin{Bmatrix} \sigma_{xx} \\ \sigma_{zz} \\ \tau_{xz} \end{Bmatrix}^{(k)} = \begin{bmatrix} C_{11}^{(k)} & C_{12}^{(k)} & 0 \\ C_{21}^{(k)} & C_{22}^{(k)} & 0 \\ 0 & 0 & C_{33}^{(k)} \end{bmatrix} \begin{Bmatrix} \varepsilon_{xx} \\ \varepsilon_{zz} \\ \gamma_{xz} \end{Bmatrix}^{(k)}, \tag{12}$$

where

$$C_{11}^{(k)} = \frac{E_x^{(k)}}{1 - \nu_{xz}^{(k)}\nu_{zx}^{(k)}}, \quad C_{12}^{(k)} = \frac{E_x^{(k)}\nu_{zx}^{(k)}}{1 - \nu_{xz}^{(k)}\nu_{zx}^{(k)}},$$
$$C_{21}^{(k)} = \frac{E_z^{(k)}\nu_{xz}^{(k)}}{1 - \nu_{xz}^{(k)}\nu_{zx}^{(k)}}, \quad C_{22}^{(k)} = \frac{E_z^{(k)}}{1 - \nu_{xz}^{(k)}\nu_{zx}^{(k)}}, \quad C_{33}^{(k)} = G_{xz}^{(k)}, \tag{13}$$

where $E_x^{(k)}$ and $E_z^{(k)}$ are Young's modulus and $v_{xz}^{(k)}$ and $v_{zx}^{(k)}$ are the Poisson's ratios. The first suffix of v denotes the direction of stress and the second, that of expansion and contraction. The following relations can be established by the reciprocal theorem:

$$E_x v_{zx} = E_z v_{xz}. \tag{14}$$

2.4. Stress resultants in terms of the expanded displacement components

Stress resultants can be derived from Eqs. (10) and (12) in terms of the expanded displacement components as

$$\overset{(n)}{N} = \sum_{m=0}^{\infty} \left\{ \overset{(n+m+1)}{C_{11}} \left[\overset{(m)}{u}_{,x} - \frac{1}{R} \overset{(m)}{w} \right] + \overset{(n+m+1)}{C_{12}} (m+1) \overset{(m+1)}{w} \right\},$$

$$\overset{(n)}{T} = \sum_{m=0}^{\infty} \left\{ \overset{(n+m+1)}{C_{21}} \left[\overset{(m)}{u}_{,x} - \frac{1}{R} \overset{(m)}{w} \right] + \overset{(n+m+1)}{C_{22}} (m+1) \overset{(m+1)}{w} \right\},$$

$$\overset{(n)}{Q} = \sum_{m=0}^{\infty} \left\{ \frac{1}{2} \overset{(n+m+1)}{C_{33}} \left[(m+1) \overset{(m+1)}{u} - \frac{m-1}{R} \overset{(m)}{u} + \overset{(m)}{w}_{,x} \right] \right\}, \tag{15}$$

where

$$\overset{(n+m+1)}{C_{ij}} = \sum_{k=1}^{K} C_{ij}^{(k)} \frac{H_{k+1}^{n+m+1} - H_k^{n+m+1}}{n+m+1} \quad (i,j = 1,2,3). \tag{16}$$

2.5. Equations of motion in terms of the expanded displacement components

The equations of motion can be expressed in terms of the expanded displacement components by using Eqs. (15) as

$$\begin{aligned} \delta \overset{(n)}{u} : \sum_{m=0}^{\infty} \Bigg\{ & \left(\overset{(n+m+1)}{C_{11}} \left[\overset{(m)}{u}_{,x} - \frac{1}{R} \overset{(m)}{w} \right] + \overset{(n+m+1)}{C_{12}} (m+1) \overset{(m+1)}{w} \right)_{,x} \\ & + \frac{n-1}{2R} \overset{(n+m+1)}{C_{33}} \left[(m+1) \overset{(m+1)}{u} - \frac{m-1}{R} \overset{(m)}{u} + \overset{(m)}{w}_{,x} \right] - \overset{(n+m+1)}{\rho} \overset{(m)}{\ddot{u}} \\ & - \frac{n}{2} \overset{(n+m)}{C_{33}} \left[(m+1) \overset{(m+1)}{u} - \frac{m-1}{R} \overset{(m)}{u} + \overset{(m)}{w}_{,x} \right] + \sum_{\ell=0}^{\infty} \overset{(n+m+\ell+1)}{\sigma_0} \overset{(m)}{u}_{,xx} \Bigg\} = 0, \end{aligned} \tag{17}$$

$$\delta \overset{(n)}{w}: \sum_{m=0}^{\infty}\left\{\frac{1}{R}\left(\overset{(n+m+1)}{C_{11}}\left[\overset{(m)}{u}_{,x}-\frac{1}{R}\overset{(m)}{w}\right]+\overset{(n+m+1)}{C_{12}}(m+1)\overset{(m+1)}{w}\right)\right.$$
$$+\frac{1}{2}\overset{(n+m+1)}{C_{33}}\left[(m+1)\overset{(m+1)}{u}-\frac{m-1}{R}\overset{(m)}{u}+\overset{(m)}{w}_{,x}\right]_{,x}-\overset{(n+m+1)}{\rho}\overset{(m)}{\ddot{w}}$$
$$\left.-n\left(\overset{(n+m)}{C_{22}}(m+1)\overset{(m+1)}{w}+\overset{(n+m)}{C_{21}}\left[\overset{(m)}{u}_{,x}-\frac{1}{R}\overset{(m)}{w}\right]\right)+\sum_{\ell=0}^{\infty}\overset{(n+m+\ell+1)}{\sigma_0}\overset{(m)}{w}_{,xx}\right\}=0. \tag{18}$$

2.6. *M*th order approximate theory

Since the fundamental equations mentioned above are complex, approximate arch theories of various orders may be considered for the present problem. A set of the following combination of displacement components for Mth ($M \geqslant 1$) order approximate equations is proposed:

$$u=\sum_{m=0}^{2M-1}\overset{(m)}{u}z^m, \qquad w=\sum_{m=0}^{2M-2}\overset{(m)}{w}z^m, \tag{19}$$

where $m = 0, 1, 2, 3, \ldots$.

The total number of the unknown displacement components is $(4M-1)$. In the above cases of $M = 1$, an assumption of plane strains in the depth direction is inherently imposed.

Another set of the governing equations of the lowest order approximate theory ($M = 1$) is derived with the use of the assumption that the normal stress σ_{zz} is zero. This theory corresponds to the Timoshenko-type arch theory with the shear correction coefficient $\kappa^2 = 1$.

3. Navier solution for simply supported circular arches

In order to show the applicability and reliability of the present one-dimensional higher order theories for the analysis of vibration and buckling problems of laminated composite circular arches, a simply supported circular arch subjected to initial axial stress is analyzed. In the following analysis, the initial axial stress σ_0 is assumed to distribute uniformly in the depth direction.

The boundary condition (11) can be expressed at the x-constant ends,

$$\overset{(n)}{u}_{,x}=0, \qquad \overset{(n)}{w}=0. \tag{20}$$

Since an arch is in a state of uniform stresses, the initial axial stress is considered to be constant during vibrating and/or buckling. Following the Navier solution procedure, displacement components that satisfy the equations of boundary conditions (20) may be expressed as

$$\overset{(n)}{u}=\sum_{r=1}^{\infty}\overset{(n)}{u_r}\cos\frac{r\pi x}{L}e^{\mathbf{i}\omega t}, \qquad \overset{(n)}{w}=\sum_{r=1}^{\infty}\overset{(n)}{w_r}\sin\frac{r\pi x}{L}e^{\mathbf{i}\omega t}, \tag{21}$$

where the displacement mode number $r = 1, 2, 3, \ldots, \infty$ and ω denotes the circular frequency; $\mathbf{i}$ is the imaginary unit.

The equations of motion are rewritten in terms of the generalized displacement components $\overset{(n)}{u}_r$ and $\overset{(n)}{w}_r$.

The dimensionless initial axial or buckling stress Λ is defined as follows:

$$\Lambda = \frac{AL^2}{\pi^2 I}\frac{\sigma_0}{E_x^{(1)}}, \tag{22}$$

where

$$A = BH, \qquad I = BH^3/12. \tag{23}$$

The dimensionless frequencies Ω and Ω_Q is defined as follows:

$$\Omega = \omega H\sqrt{\rho^{(1)}/E_x^{(1)}}, \qquad \Omega_Q = \Omega\sqrt{12}(L/H)^2. \tag{24}$$

4. Eigenvalue problem for vibration and buckling problems

The equations of motion (17) and (18) can be rewritten by collecting the coefficients for the generalized displacements of any fixed value r. The generalized displacement vector $\{\mathbf{U}\}$ is expressed as

$$\{\mathbf{U}\}^{\mathrm{T}} = \{\overset{(0)}{u}_r, \ldots, \overset{(2M-1)}{u}_r; \overset{(0)}{w}_r, \ldots, \overset{(2M-2)}{w}_r\}. \tag{25}$$

The dynamic equation can be expressed as the following eigenvalue problem:

$$([\mathbf{K}] - \Omega^2[\mathbf{M}])\{\mathbf{U}\} = \{0\}, \tag{26}$$

where matrix [**K**] denotes the stiffness matrix which may contain the terms of the initial axial stress and matrix [**M**], the mass matrix.

For buckling problems, the natural frequency vanishes and the stability equation can be expressed as the following eigenvalue problem:

$$([\mathbf{K}] + \Lambda[\mathbf{S}])\{\mathbf{U}\} = \{0\}, \tag{27}$$

where matrix [**K**] denotes the stiffness matrix and matrix [**S**], the geometric-stiffness matrix due to the initial axial stress.

The number of eigenvalues is the same as that of the components of the generalized displacement vector for each displacement mode number of r. Although all the eigenvalues and eigenvectors can be computed, the dominant eigenvalue which corresponds to the minimum natural frequency or the critical buckling stress is of great concern. When the lowest natural frequency vanishes, the axial stress reduces to the critical buckling stress of the arch.

5. Determination of modal stress distribution

Although the transverse stress components can be calculated from the constitutive relations, these stresses may not satisfy the continuity conditions at the interface between layers and stress boundary conditions on the top and bottom surfaces of a laminated arch. Axial stress component

has no reference to the surface boundary conditions and can be obtained by the constitutive relations. With the use of the axial stress component, therefore, transverse stress components are determined by integrating the equations of motion of three-dimensional elastic continuum, and satisfying the stress boundary conditions on the top and bottom surfaces of an arch and the continuity conditions at the interfaces between layers. The modal axial stress of the kth layer can be derived in terms of the expanded displacement components by introducing the strain–displacement relations (4) into the constitutive relations (12). The modal transverse stresses of the kth layer are obtained by integrating the three-dimensional equations of motion in the depth direction starting from the top (or bottom) surface of the laminated arch as follows:

$$\tau_{xz}^{(k)} = -\int_{H_k}^{z}\left(\sigma_{xx,x} - \frac{1}{R}\tau_{xz} - \rho\ddot{u}\right)\mathrm{d}z + C_1^{(k)}(x),$$
$$\sigma_{zz}^{(k)} = -\int_{H_k}^{z}\left(\tau_{xz,x} + \frac{1}{R}\sigma_{xx} - \rho\ddot{w}\right)\mathrm{d}z + C_2^{(k)}(x), \tag{28}$$

where $C_1^{(k)}$ and $C_2^{(k)}$ are integral constants (functions of x) obtained from the stress conditions on the top and bottom surfaces of kth layer. If the boundary conditions of transverse stresses are prescribed on one of the top or bottom surfaces, the stress boundary conditions on the other surface can be satisfied through the equations of motion (17) and (18). Because of the discontinuity of the axial stress at layer interfaces, the integration is performed in a piecewise manner. The modal stress components in the kth layer of laminated composite arches can be expressed as follows:

$$\sigma_{xx}^{(k)} = \sum_{n=0}^{\infty}[F_1]^{(k)}z^n, \tag{29}$$

$$\tau_{xz}^{(k)} = -\sum_{n=0}^{\infty}\left[F_{1,x} - \frac{1}{R}F_2 + \rho\omega^2\overset{(n)}{u}\right]^{(k)}\frac{[z^{n+1} - H_k^{n+1}]}{n+1} + \tau_{xz}^{(k-1)}|_{z=H_k}, \tag{30}$$

$$\sigma_{zz}^{(k)} = \sum_{n=0}^{\infty}\left[F_{1,xx} - \frac{1}{R}F_{2,x} + \rho\omega^2\overset{(n)}{u}_{,x}\right]^{(k)}\left[\frac{z^{n+2} - H_k^{n+2}}{(n+1)(n+2)} - \frac{H_k^{n+1}(z - H_k)}{n+1}\right]$$
$$-\sum_{n=0}^{\infty}\left[\frac{1}{R}F_1 + \rho\omega^2\overset{(n)}{w}\right]^{(k)}\frac{[z^{n+1} - H_k^{n+1}]}{n+1} - \tau_{xz,x}^{(k-1)}|_{z=H_k}[z - H_k] + \sigma_{zz}^{(k-1)}|_{z=H_k}, \tag{31}$$

where

$$F_1 \equiv C_{11}\left(\overset{(n)}{u}_{,x} - \frac{1}{R}\overset{(n)}{w}\right) + (n+1)C_{12}\overset{(n+1)}{w},$$
$$F_2 \equiv \frac{1}{2}C_{33}\left[(n+1)\overset{(n+1)}{u} - \frac{n-1}{R}\overset{(n)}{u} + \overset{(n)}{w}_{,x}\right]. \tag{32}$$

Table 1
Convergence of first four natural frequencies of cross-ply laminated composite circular arches ($K = 2 : [0^\circ/90^\circ]$, $K = 3 : [0^\circ/90^\circ/0^\circ]$; $\Omega_Q = \Omega\sqrt{12}(L/H)^2$, $L/R = 1$; Material 1)

K	H/R	E_L/E_T	r	$M = 1$	$M = 2$	$M = 3$	$M = 4$	$M = 5$
2	0.1	15	1	3.8159	3.7395	3.7260	3.7250	3.7248
			2	15.7705	15.2580	15.0951	15.0853	15.0825
			3	32.5229	31.0216	30.4909	30.4643	30.4554
			4	51.8449	48.8399	47.8154	47.7747	47.7581
		40	1	3.1472	3.0555	3.0146	3.0115	3.0107
			2	12.3988	11.6107	11.2336	11.2120	11.2043
			3	24.3533	22.1165	21.1931	21.1528	21.1321
			4	37.2798	33.1924	31.7928	31.7496	31.7122
	0.2	15	1	3.4179	3.3028	3.2687	3.2662	3.2655
			2	12.3373	11.6231	11.3904	11.3794	11.3751
			3	22.7556	21.0912	20.6415	20.6301	20.6220
			4	33.4636	30.7870	30.2088	30.2013	30.1910
		40	1	2.6903	2.5075	2.4281	2.4226	2.4208
			2	8.9079	7.9087	7.5817	7.5695	7.5603
			3	15.5408	13.5874	13.1502	13.1423	13.1246
			4	22.0939	19.3454	18.9165	18.9074	18.8840
3	0.1	15	1	7.4498	7.2863	7.2795	7.2790	7.2788
			2	26.6113	25.5198	25.4892	25.4868	25.4858
			3	48.2191	45.8053	45.7155	45.7124	45.7109
			4	69.8673	66.2404	66.0316	66.0290	66.0275
		40	1	6.4791	6.2193	6.2079	6.2071	6.2068
			2	19.8053	18.7442	18.6993	18.6980	18.6974
			3	33.0725	31.3681	31.2328	31.2312	31.2305
			4	45.9651	43.9042	43.6116	43.6032	43.6019
	0.2	15	1	5.9072	5.6256	5.6097	5.6089	5.6087
			2	16.9526	16.0337	15.9675	15.9660	15.9654
			3	27.6665	26.3487	26.1705	26.1653	26.1635
			4	38.0762	36.5950	36.2550	36.2339	36.2289
		40	1	4.3991	4.1191	4.1013	4.1006	4.1004
			2	11.1602	10.6243	10.5465	10.5436	10.5426
			3	17.5535	16.9774	16.8008	16.7836	16.7797
			4	23.8042	23.2651	23.0010	22.9531	22.9430

6. Numerical examples and results

6.1. Numerical examples

The effects of transverse shear and normal stresses and rotatory inertia on natural frequencies and/or buckling stresses of a simply supported cross-ply laminated composite arch subjected to initial axial stress are studied through the numerical examples. The following sets of orthotropic material constants of each layer are taken to be the same in all the layers, but the fibre orientations may be different among layers:

Table 2
Comparison of natural frequencies of cross-ply laminated composite circular arches ($K = 2:[0^\circ/90^\circ]$; $\Omega_Q = \Omega\sqrt{12}(L/H)^2$, $L/R = 1$, $r = 1$–4; Material 1)

	Qatu				Present			
H/R	$r = 1$	$r = 2$	$r = 3$	$r = 4$	$r = 1$	$r = 2$	$r = 3$	$r = 4$
$E_L/E_T = 1$								
0.01	8.4508	37.980	87.229	156.07	8.4506	37.9794	87.2294	156.0802
0.02	8.4478	37.919	86.909	155.06	8.4470	37.9173	86.9118	155.0799
0.05	8.4270	37.504	84.790	148.58	8.4244	37.4931	84.8056	148.6986
0.10	8.3546	36.153	78.546	131.57	8.3366	36.1113	78.5861	131.8830
0.20	8.0874	32.122	63.760	98.806	8.0221	31.9905	63.7929	99.2398
$E_L/E_T = 15$								
0.01	4.0094	18.000	41.286	73.738	4.0107	18.0026	41.2798	73.6985
0.02	3.9855	17.839	40.681	72.095	3.9903	17.8345	40.6259	71.8909
0.05	3.9109	17.089	37.667	64.041	3.9099	17.0177	37.3029	63.0335
0.10	3.7419	15.329	31.300	49.452	3.7248	15.0825	30.4554	47.7581
0.20	3.3312	11.808	21.481	31.295	3.2655	11.3751	20.6220	30.1910
$E_L/E_T = 40$								
0.01	3.4108	15.298	35.034	62.438	3.4122	15.2904	34.9639	62.1867
0.02	3.3871	15.093	35.220	60.178	3.3875	15.0416	33.9130	59.2143
0.05	3.2932	14.111	30.283	50.017	3.2771	13.7862	28.9378	46.8347
0.10	3.0814	11.964	23.180	35.118	3.0107	11.2043	21.1321	31.7122
0.20	2.5935	3.3979	14.446	20.425	2.4208	7.5603	13.1246	18.8840

Ref. [4]: Moderately thick beam theory (Reissner–Naghdi type of shell theory, Kirchhoff hypothesis). Present solutions: $M = 5$.

Material 1:

$$E_L/E_T = open, \quad G_{LT}/E_T = G_{TT}/E_T = 0.5, \quad v_{LT} = 0.25. \tag{33}$$

Material 2:

$$E_L = 144.8 \text{ GPa}, \ E_T = 9.65 \text{ GPa}, \ G_{LT} = 4.14 \text{ GPa}, \ G_{TT} = 3.45 \text{ GPa}, \ v_{LT} = 0.3. \tag{34}$$

The lower suffices L and T signify the direction parallel to the fibres and the transverse direction, respectively. The fibre orientations of the different laminates alternate between 0° and 90° with respect to the x-axis. The thickness of each layer is identified for the 0° and 90° layers in the laminates. Both symmetric and antisymmetric laminations with respect to the central axis are considered. In the symmetrical laminates having an odd number of layers, the 0° layers are at the outer surfaces of the laminate. The initial axial stress $\sigma_0^{(k)}$ is identical in each layer. The mass density is also assumed to be uniform in the depth direction, i.e., $\rho^{(1)}, \rho^{(2)}, \ldots, \rho^{(k)}$ are identical. All the numerical results are obtained for the case of plane stress in the width direction and are shown in the dimensionless quantities. The absolute values of buckling stresses are shown in the following results.

Table 3
Comparison of natural frequencies of cross-ply laminated composite circular arches ($K = 2:[0^\circ/90^\circ]$; $\Omega_Q = \Omega\sqrt{12}(L/H)^2$, $L/H = 100$, $r = 1-4$; Material 1)

	Qatu				Present			
L/R	$r=1$	$r=2$	$r=3$	$r=4$	$r=1$	$r=2$	$r=3$	$r=4$
$E_L/E_T = 1$								
0.0	9.8702	39.491	88.892	158.12	9.8683	39.4570	88.7182	157.5722
0.1	9.8549	39.475	88.876	158.11	9.8533	39.4420	88.7032	157.5573
0.2	9.8102	39.431	88.830	158.06	9.8084	39.3971	88.6583	157.7512
0.3	9.7364	39.356	88.757	157.99	9.7340	39.3225	88.5834	157.4375
0.5	9.4993	39.116	88.516	157.16	9.4987	39.0835	88.3442	157.1982
0.8	8.9473	38.538	87.935	157.16	8.9429	38.5064	87.7631	156.6161
1.0	8.4516	38.000	87.335	156.42	8.4506	37.9794	87.2294	156.0802
$E_L/E_T = 15$								
0.0	4.7037	18.810	42.320	75.222	4.7010	18.7784	42.1552	74.7057
0.1	4.6936	18.795	42.295	75.181	4.6919	18.7635	42.1307	74.6680
0.2	4.6707	18.767	42.255	75.131	4.6687	18.7343	42.0921	74.6162
0.3	4.6348	18.721	42.198	75.059	4.6314	18.6911	42.0393	74.5503
0.5	4.5176	18.593	42.049	74.881	4.5159	18.5625	41.8915	74.3763
0.8	4.2483	18.296	41.721	74.509	4.2470	18.2665	41.5655	74.0109
1.0	4.0115	18.030	41.431	74.188	4.0107	18.0026	41.2798	73.6985
$E_L/E_T = 40$								
0.0	4.0072	16.024	36.040	64.061	4.0014	15.9568	35.7219	63.0640
0.1	3.9938	16.011	36.017	64.021	3.9935	15.9434	35.6996	63.0296
0.2	3.9758	15.980	35.985	63.976	3.9735	15.9179	35.6652	62.9832
0.3	3.9442	15.944	35.933	63.918	3.9416	15.8804	35.6189	62.9249
0.5	3.8432	15.831	35.805	63.757	3.8429	15.7697	35.4904	62.7726
0.8	3.6179	15.576	35.521	63.433	3.6136	15.5160	35.2093	62.4560
1.0	3.4153	15.349	35.271	63.156	3.4122	15.2904	34.9639	62.1867

Ref. [4]: Moderately thick beam theory. Present solutions: $M = 5$.

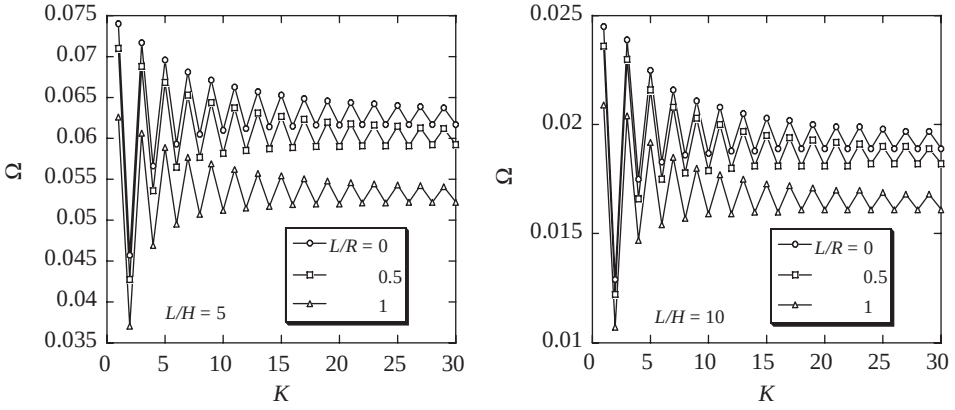

Fig. 2. Natural frequency Ω versus number of layers K (Ω_1, $L/H = 5, 10$, $K = 1-30:[0^\circ/90^\circ/0^\circ/90^\circ/\cdots]$; Material 2).

Table 4
Comparison of natural frequencies of cross-ply laminated composite beams ($K = 4:[0°/90°/90°/0°]$; $\Omega_Q = \Omega\sqrt{12}(L/H)^2$, $r = 1-7$; Material 2)

Mode number	$L/H = 10$			$L/H = 15$			
	Ref. [11]	Ref. [12]	Present	Ref. [13]	Ref. [14]	Ref. [15]	Present
1	2.3189	2.3194	2.3136	2.5023	2.5024	2.4959	2.4953
2	7.0171	7.0029	7.0044	8.4812	8.4813	8.4663	8.4657
3	12.132	12.037	12.0980	15.7558	15.7559	15.7599	15.7622
4	17.301	17.015	17.2013	23.3089	17.2591[a]	—	23.3858
5	22.533	21.907	22.2857	30.8386	23.3093	—	31.0535
6	—	23.337[1]	22.5422[1]	—	30.8391	—	34.1496[1]
7	27.881	26.736	27.3628	—	—	—	38.7030

Ref. [11]: Third order shear deformation theory (immovable hinged ends). Ref. [12]: First order shear deformation theory ($\kappa^2 = 5/6$, immovable hinged ends). Refs. [13–15]: First order shear deformation theory ($\kappa^2 = 5/6$). Present solutions: $M = 5$.

[a] The corresponding frequency did not exist in the present analysis.

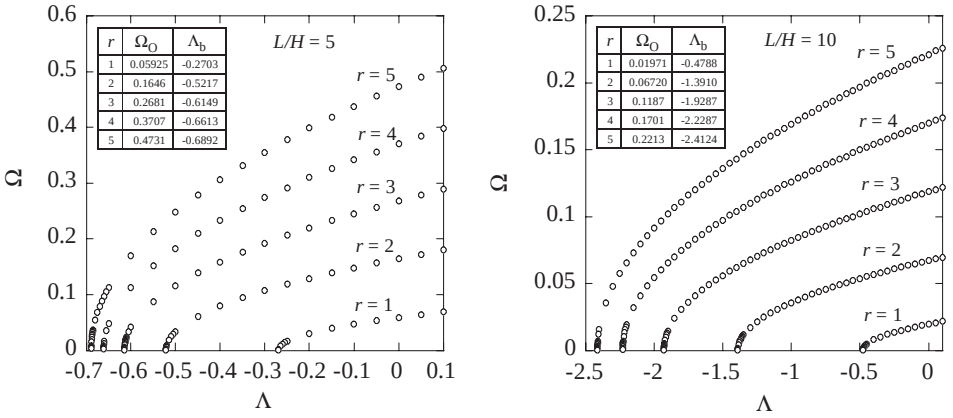

Fig. 3. Natural frequency Ω versus axial stress Λ curves (Ω_1, $L/R = 1$, $K = 4:[0°/90°/90°/0°]$; Material 2).

6.2. Convergence of first four natural frequencies

In order to verify the accuracy of the present solutions, convergences of the first four natural frequencies of cross-ply laminated composite circular arches without initial axial stress are examined in Table 1. Antisymmetric two-layer and symmetric three-layer arches of Material 1 are considered. It is noticed that the proper order of the present higher order approximate theories may be estimated according to the level of curvature parameter H/R and orthotropy ratio E_L/E_T. Since the present results for $M = 1$–5 converge accurately enough within the present order of approximate theories, only the numerical results for $M = 5$ are discussed in the following.

6.3. Comparison of natural frequencies with those of existing solutions

Comparisons of natural frequencies with existing results are also performed for simply supported cross-ply laminated composite arches of Material 1. For two-layer antisymmetric laminates $[0^\circ/90^\circ]$ of $L/R = 1$, the first four natural frequencies are compared with Qatu's results [4] in Table 2. A good agreement is obtained with the reference for this case, while a considerable difference can be noticed for higher frequencies of laminated arches with high ratio of axial modulus to transverse shear

Table 5
Natural frequencies and buckling stresses of laminated composite circular arches ($\Omega, \Lambda_b, L/H = 5, r = 1$; Material 2)

	Mode number	$[0^\circ/90^\circ]$		$[0^\circ/90^\circ/0^\circ]$		$[0^\circ/90^\circ/90^\circ/0^\circ]$	
L/R		Ω	Λ_b	Ω	Λ_b	Ω	Λ_b
0	1	0.04570	0.1608	0.07165	0.3953	0.07004	0.3778
	2	0.3589	9.9190	0.4967	18.9932	0.4255	13.9412
0.5	1	0.04271	0.1405	0.06875	0.3639	0.06720	0.3477
	2	0.3758	10.8751	0.5023	19.4242	0.4304	14.2637
1.0	1	0.03704	0.1056	0.06062	0.2829	0.05925	0.2703
	2	0.3975	12.1665	0.5180	20.6592	0.4442	15.1950

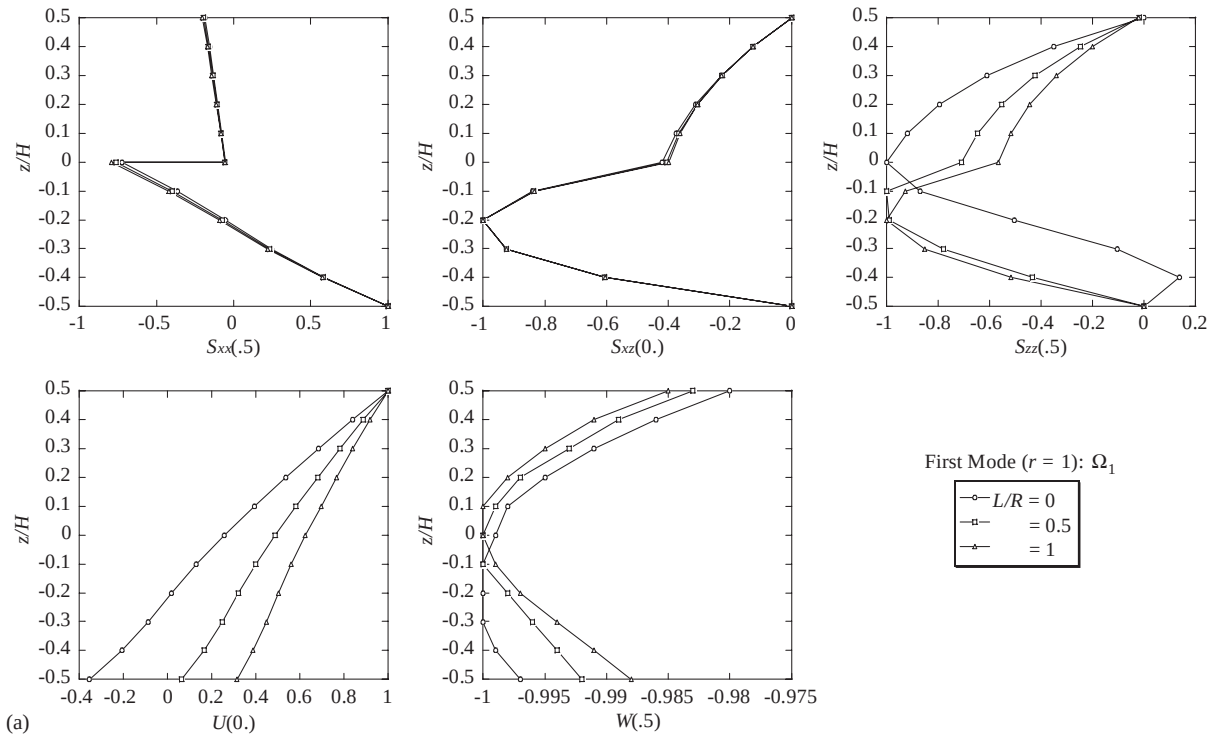

Fig. 4. (a) Modal displacement and stress distributions of two-layer cross-ply laminated composite circular arches (Ω_1, $L/H = 5$, $K = 2:[0^\circ/90^\circ]$; Material 2). (b) Modal displacement and stress distributions of two-layer cross-ply laminated composite circular arches (Ω_2, $L/H = 5$, $K = 2:[0^\circ/90^\circ]$; Material 2).

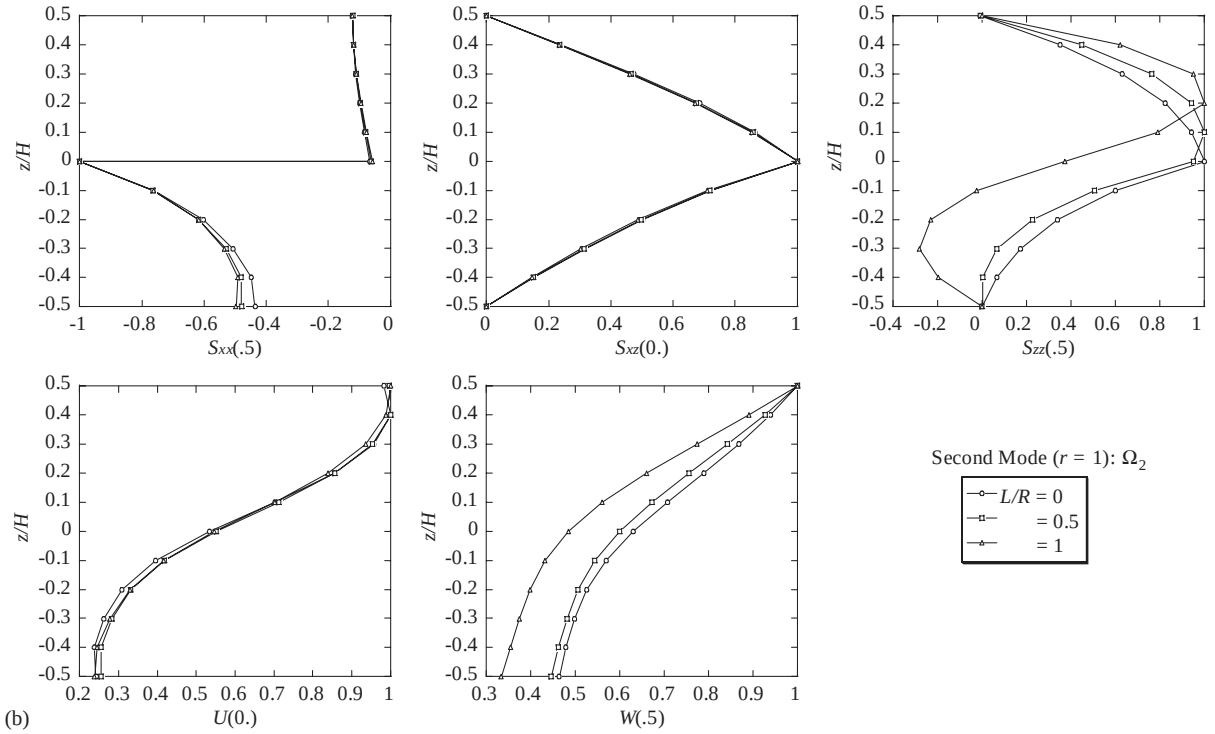

Fig. 4 (*continued*).

modulus E_L/E_T due to the effects of transverse shear and normal stresses. Comparisons with existing results [4], which are also performed for simply supported antisymmetric $[0^\circ/90^\circ]$ cross-ply laminated composite arches with the depth parameter $L/H = 100$, are shown in Table 3.

In Table 4, the first seven natural frequencies of four-layer simply supported symmetric cross-ply laminated composite beams of Material 2 are compared with the results in Refs. [10–14]. The superscript on the right shoulder of natural frequency in Table 4 is the longitudinal vibration mode number r. A good agreement is obtained with the references for symmetric cross-ply laminated composite beams.

6.4. Fundamental natural frequencies with respect to number of layers

Fig. 2 shows the variation of fundamental natural frequencies Ω of simply supported cross-ply laminated composite circular arches with respect to number of layers $K = 1$–30. The material properties of the individual layers are given by Material 2. Since the total number of unknowns of the present global higher order theory does not increase as the number of layers increases, multilayered composite circular arches with a large number of layers can be analyzed without difficulty. For small number of layers, the natural frequency is influenced largely by the number of layers and stacking sequences. However, for large number of layers, the natural frequency does not change and approaches a constant value. The feature of the anisotropy effects becoming stabilized as the number of layers increases can also be noticed for higher frequencies.

6.5. Buckling stresses of laminated composite circular arches

The buckling stresses can be calculated usually through the stability equation (27) as eigenvalue problems. Another method to obtain the buckling stresses of laminated composite arches subjected to initial axial stress is to compute natural frequencies by increasing the absolute value of compressive stresses till the corresponding natural frequency vanishes.

In the case of a simply supported arch subjected to initial axial stress Λ, the natural frequency Ω_a can be expressed explicitly with reference to the natural frequency Ω_0 of arches without axial stress. The relation between Ω_a and Ω_0 can be obtained from a comparison of the equations of motion as follows:

$$\Omega_a^2 = \Omega_0^2 + \frac{r^2\pi^4}{12}\left(\frac{H}{L}\right)^4 \Lambda. \tag{35}$$

When the natural frequency Ω_a vanishes under the initial axial stress, elastic buckling occurs and the buckling stress Λ_b relates with the natural frequency Ω_0 as

$$\Lambda_b = -\frac{12}{r^2\pi^4}\left(\frac{L}{H}\right)^4 \Omega_0^2. \tag{36}$$

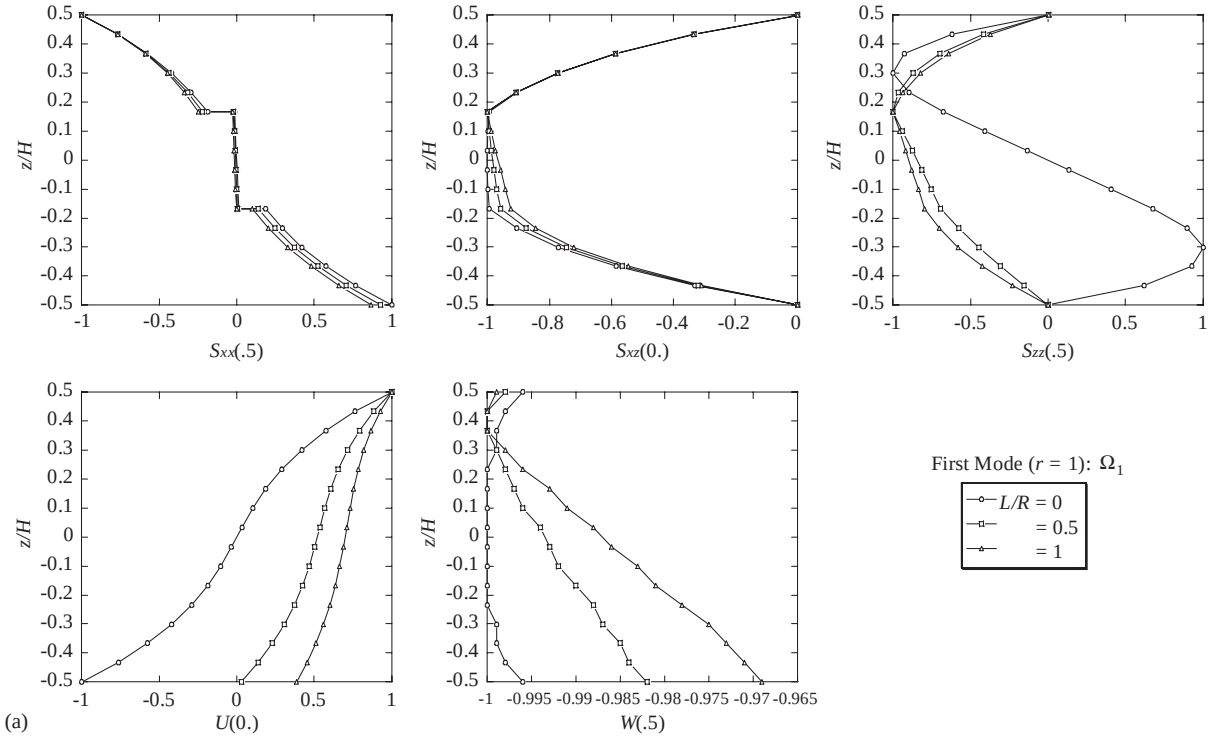

Fig. 5. (a) Modal displacement and stress distributions of three-layer cross-ply laminated composite circular arches (Ω_1, $L/H = 5$, $K = 3:[0^\circ/90^\circ/0^\circ]$; Material 2). (b) Modal displacement and stress distributions of three-layer cross-ply laminated composite circular arches (Ω_2, $L/H = 5$, $K = 3:[0^\circ/90^\circ/0^\circ]$; Material 2).

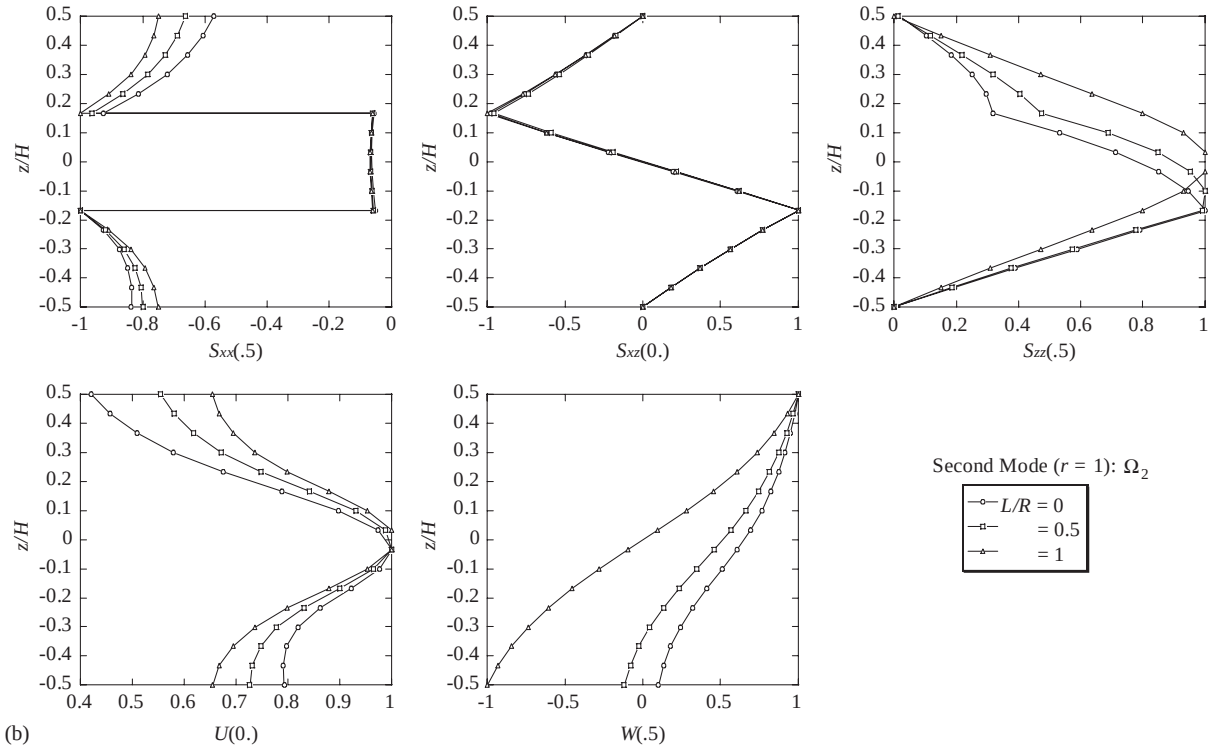

Fig. 5 (*continued*).

The buckling stresses of simply supported laminated composite arches subjected to initial axial stress can be predicted from the natural frequency of the arches without axial stress.

For symmetric four-layer laminated composite arches of Material-2 with the curvature parameter $L/R = 1$ and the thickness parameter $L/H = 5$ and 10, the lowest natural frequencies are plotted with respect to the initial axial stress in Fig. 3. The figures show the effects of initial axial stress on the frequency curves for the first five displacement modes of $r = 1$–5. When the natural frequencies go to zero, the initial axial stress reduces to the buckling stresses of the arch. In Table 5, the first two natural frequencies and the corresponding buckling stresses of simply supported cross-ply laminated composite arches are shown for symmetric and antisymmetric laminates of $L/H = 5$. It can be seen that relation (36) is established between the buckling stress and natural frequency in Table 5.

6.6. Modal displacement and stress distributions

For two-, three- and four-layer laminated composite circular arches of Material-2 with the thickness parameter $L/H = 5$, the distributions of modal displacements and stresses associated with the first two natural frequencies Ω_1 and Ω_2 for the fundamental displacement mode $r = 1$ are shown in Figs. 4a–b, 5a–b and 6a–b, respectively. The lower natural frequency Ω_1 is for predominantly bending mode with some shear deformation, whereas the upper frequency Ω_2 is for predominantly axial mode. The modal displacement and stress distributions in the x direction

follow harmonic functions. In the figures, the through-the-thickness distributions of modal displacements and stresses are normalized by their maximum absolute values. The normal stresses $S_{xx}(\xi) \equiv s_{xx}/|s_{xx}|_{max}$ and $S_{zz}(\xi) \equiv s_{zz}/|s_{zz}|_{max}$, and the transverse displacement $W(\xi) \equiv w/|w|_{max}$ are calculated at $\xi = x/a = 0.5$. The transverse shear stress $S_{xz}(\xi) \equiv s_{xz}/|s_{xz}|_{max}$ and the in-plane displacement $U(\xi) \equiv u/|u|_{max}$ are calculated at $\xi = 0.0$. The stress boundary conditions at the top and bottom surfaces of the arch and the continuity conditions at the interfaces between layers are satisfied accurately.

The corresponding natural frequencies and buckling stresses (with minus sign) to the modal displacement and stress components in Figs. 4–6 are shown in Table 5.

7. Conclusions

Natural frequencies and buckling stresses of simply supported multilayered composite circular arches have been analyzed by using a global higher order arch theory. In order to analyze the complete effects of higher order deformations on the natural frequencies and buckling stresses of cross-ply laminated composite circular arches, various orders of the expanded approximate laminate theories have been presented. It is shown through the numerical examples that the

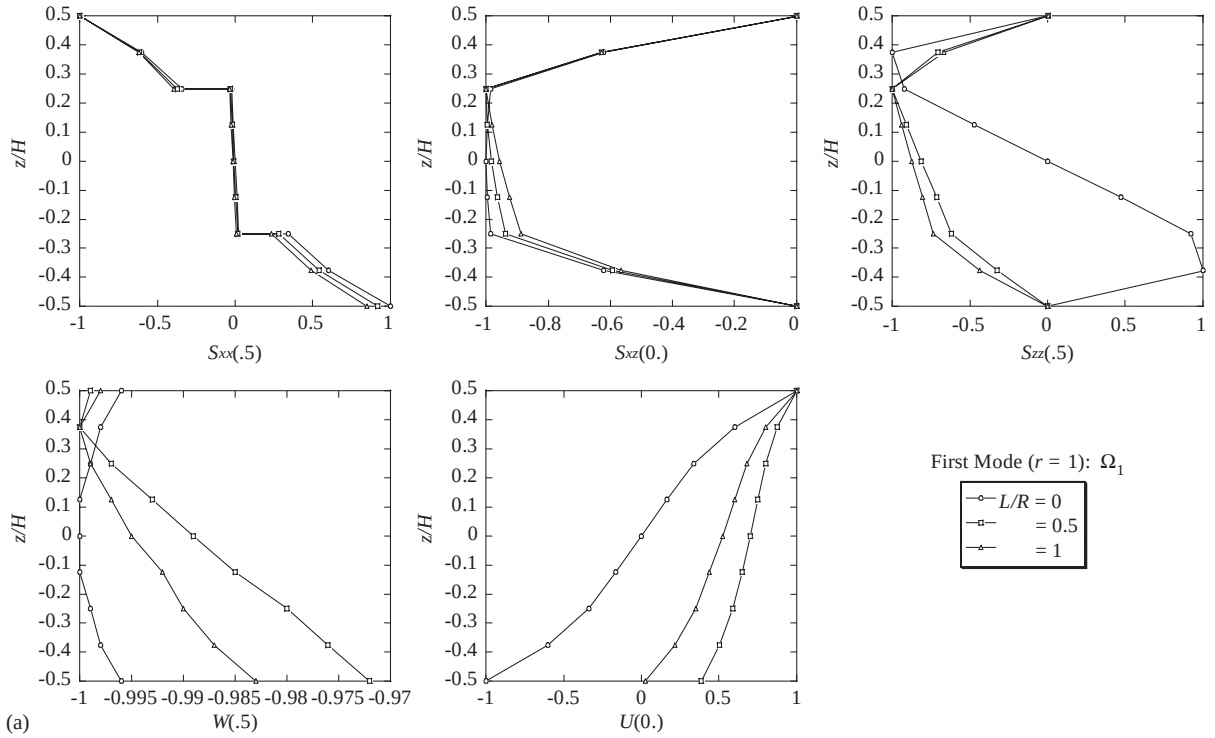

Fig. 6. (a) Modal displacement and stress distributions of four-layer cross-ply laminated composite circular arches (Ω_1, $L/H = 5$, $K = 4:[0^\circ/90^\circ/90^\circ/0^\circ]$; Material 2). (b) Modal displacement and stress distributions of four-layer cross-ply laminated composite circular arches (Ω_2, $L/H = 5$, $K = 4:[0^\circ/90^\circ/90^\circ/0^\circ]$; Material 2).

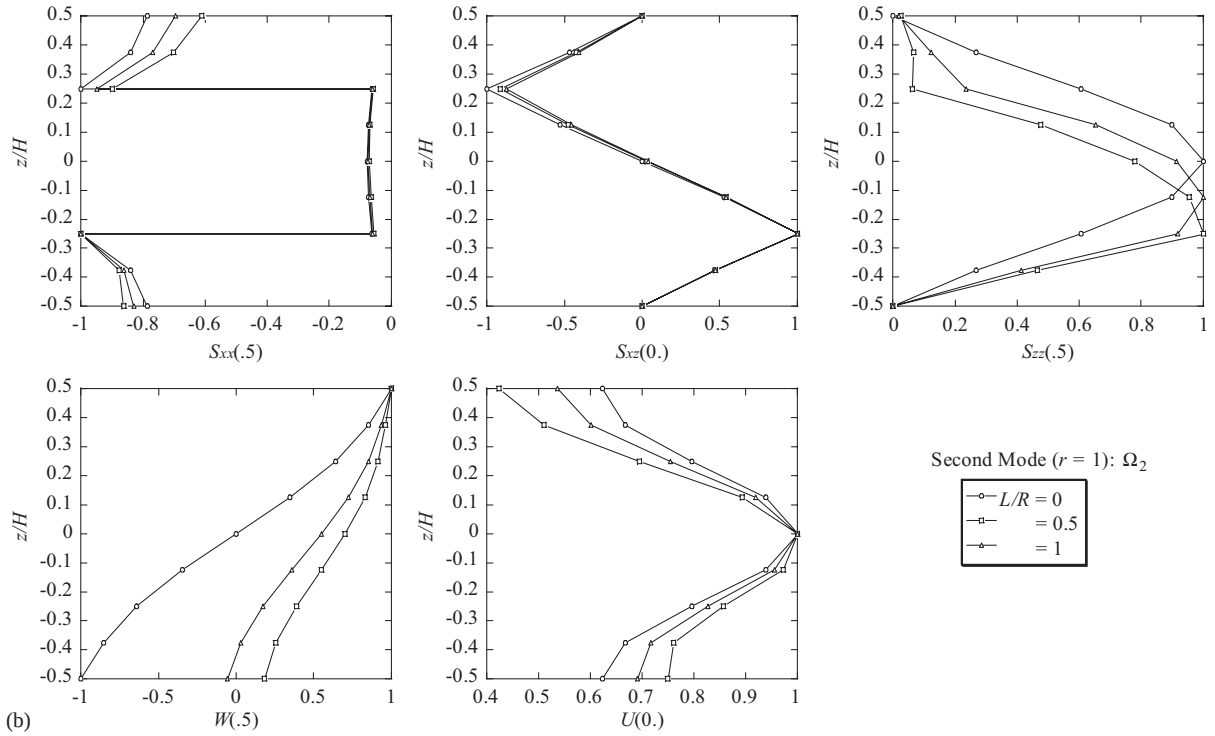

Fig. 6 (*continued*).

present global higher order theories can provide accurate results for natural frequencies and buckling stresses of general cross-ply laminated composite circular arches. The total number of unknowns is not dependent on the number of layers in any multilayered arches. It should be pointed out that the present theory has the advantage of predicting natural frequencies and buckling stresses of multilayered composite arches without increasing the unknowns involved as the number of layers increases.

The distribution of modal displacements and stresses in the depth direction has also been obtained accurately in the ply level. The modal transverse shear and normal stresses have been obtained by integrating the three-dimensional equations of motion in the depth direction. The stress boundary conditions at the top and bottom surfaces of the arch and the continuity conditions at the interfaces between layers have been satisfied.

It has been shown that a global higher order arch theory can predict not only the natural frequency and buckling stress but also the accurate distribution of modal displacements and stress components in multilayered composite arches.

References

[1] P.P.A. Laura, M.J. Maurizi, Recent research on vibrations of arch-type structures, Shock and Vibration Digest 19 (1987) 6–9.

[2] P. Childamparam, A.W. Leissa, Vibrations of planar curved beams, rings, and arches, Applied Mechanics Reviews 46 (9) (1993) 467–483.
[3] M.S. Qatu, In-plane vibration of slightly curved laminated composite beams, Journal of Sound and Vibration 159 (2) (1992) 327–338.
[4] M.S. Qatu, Theories and analysis of thin and moderately thick laminated composite curved beams, International Journal of Solids and Structures 30 (20) (1993) 2743–2756.
[5] M.S. Qatu, A.A. Elsharkawy, Vibration of laminated composite arches with deep curvature and arbitrary boundaries, Computers and Structures 47 (2) (1993) 305–311.
[6] Y.P. Tseng, C.S. Huang, M.S. Kao, In-plane vibration of laminated curved beams with variable curvature by dynamic stiffness analysis, Composite Structures 50 (2000) 103–114.
[7] H. Matsunaga, In-plane vibration and stability of shallow circular arches subjected to axial forces, International Journal of Solids and Structures 33 (4) (1996) 469–482.
[8] H. Matsunaga, Effects of higher-order deformations on in-plane vibration and instability of thick circular rings, Acta Mechanica 124 (1–4) (1997) 47–61.
[9] H. Matsunaga, Vibration and buckling of multilayered composite beams according to higher order deformation theories, Journal of Sound and Vibration 246 (1) (2001) 47–62.
[10] Y. Yokoo, H. Matsunaga, A general nonlinear theory of elastic shells, International Journal of Solids and Structures 10 (2) (1974) 261–274.
[11] M.P. Singh, A.S. Abdelnaser, Random response of symmetric cross-ply composite beams with arbitrary boundary conditions, American Institute of Aeronautics and Astronautics Journal 30 (4) (1992) 1081–1088.
[12] A. Abramovich, H. Livshits, Free vibrations of non-symmetric cross-ply laminated composite beams, Journal of Sound and Vibration 176 (5) (1994) 597–612.
[13] K. Chandrasekhara, K. Krishnamurthy, S. Roy, Free vibration of composite beams including rotary inertia and shear deformation, Composite Structures 14 (1990) 269–279.
[14] M. Eisengerger, H. Abramovich, O. Shulepov, Dynamic stiffness analysis of laminated beams using a first-order shear deformation theory, Composite Structures 31 (1995) 265–271.
[15] V. Yildirim, E. Kiral, Investigation of the rotary inertia and shear deformation effects on the out-of-plane bending and torsional natural frequencies of laminated beams, Composite Structures 49 (2000) 313–320.